

Introduction

Investigating organic matter (OM) in primitive interplanetary materials can constrain prebiotic evolution in the early Solar System. Carbonaceous chondrites (CCs) preserve primitive components from presolar, nebular to parent body origins. Organic material occurs in the matrices of CCs in both soluble (SOM) [1] and insoluble form (IOM) [2], with total organic carbon (TOC) abundances reaching up to ~3-4 wt% in the most primitive CCs [3], such as Ivuna-type (CI) chondrites. As well as being important for studying the evolution of OM from the early Solar System, they are relevant to the study of asteroid 162173 Ryugu samples from the Hayabusa-2 mission that are of CI composition.

Microanalytical studies of bulk meteorite SOM and IOM separates coupled with their characterization *in situ* provide a comprehensive account of OM [4]. Studies of OM *in situ* reveal its morphology, organic functional chemical variation, and distribution amongst inorganic materials. This requires techniques such as synchrotron based soft X-Ray scanning transmission microscopy (STXM) coordinated with scanning electron microscopy (SEM) and transmission electron microscopy (TEM) with samples prepared using e.g. focused ion beam (FIB) techniques. Studies have shown the presence of distinct micron to submicron organic particles (e.g., [5]) consistent with IOM. They mostly display aromatic-carbonyl-carboxyl carbon K-edge X-Ray absorption near edge structure (XANES) spectra by STXM. In addition, diffuse OM [6], aromatic-poorer and carboxylic-rich than organic particles occur within hydrated silicates, namely phyllosilicate in CI chondrites. Diffuse OM is consistent with a complex mixture of both SOM and IOM [5, 6].

As electron microscopy techniques are getting better with e.g. modern aberration corrected TEM coupled with electron energy spectroscopy (EELS), similar results to XANES could be possible but at higher spatial resolution and faster data acquisition than synchrotron-based STXM-XANES coordinated separately with TEM. In this context, we present the results of a comparative C K-edge XANES and EELS study of OM in the CI chondrite, Ivuna. Two adjacent ~100 nm thick lamella were prepared by FIB-SEM (Fig. 1). Lamella 1 (Fig. 2) was prepared using Xe-plasma FIB-SEM with the Helios 5 Hydra DualBeam (CEITEC, Masaryk University, Czechia) and analysed by TEM-EELS with the JEOL ARM200CF (ePSCl, Diamond Light Source, UK), followed by STXM-XANES at Beamline BL19A of the KEK Photon Factory, Japan. Lamella 2 (Fig. 5) was prepared by Xe-plasma FIB-SEM with the TESCAN AMBER X (TESCAN ORSAY holding a.s., Brno, Czechia) followed by STXM-XANES (i.e. no TEM) at the photon factory [7].

Lamella 1 – TEM-EELS first

SEM-TLD (5 kV)

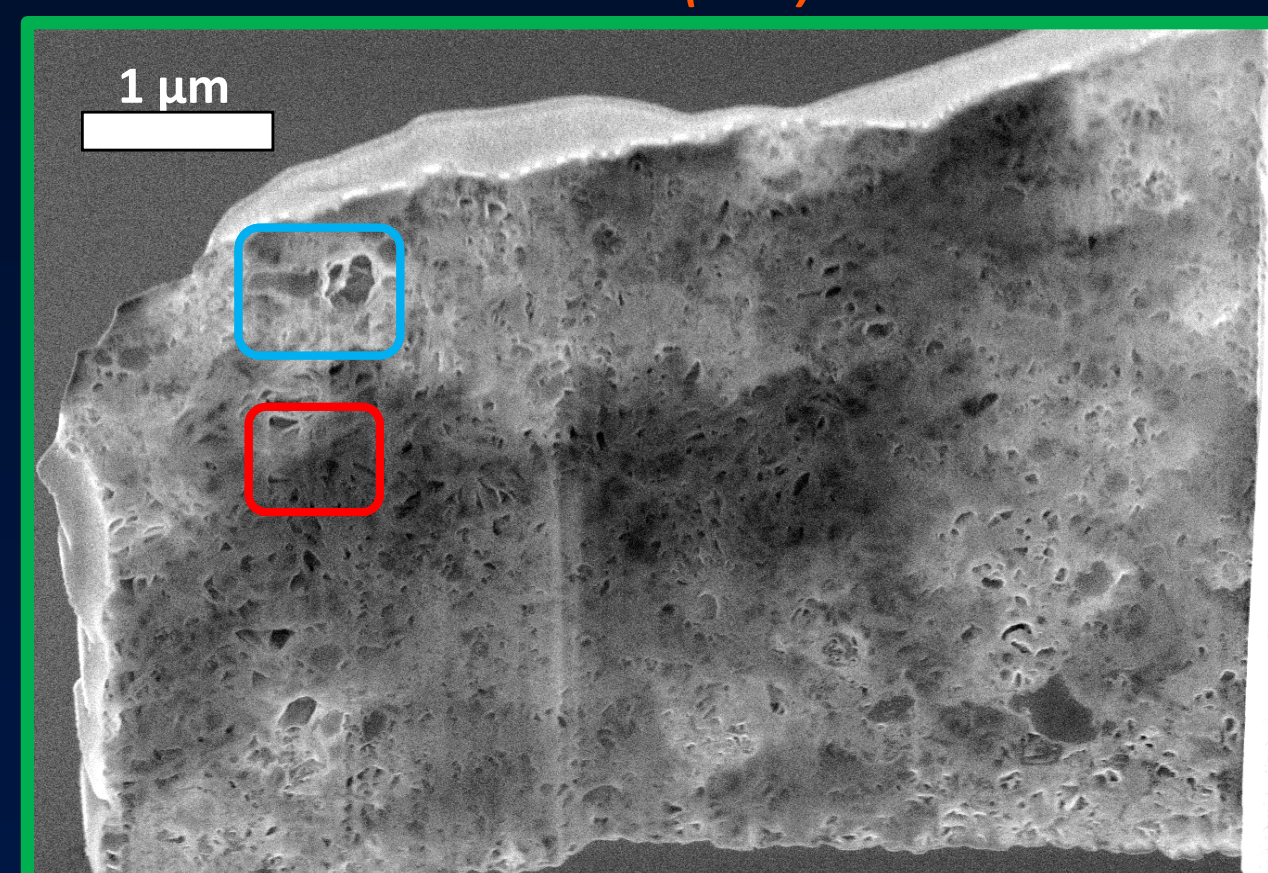


Figure 2: SEM TLD Image of Ivuna lamella which had S/TEM and EELS performed on it followed by STXM.

Ivuna Sample

SEM-ETD (5 kV)

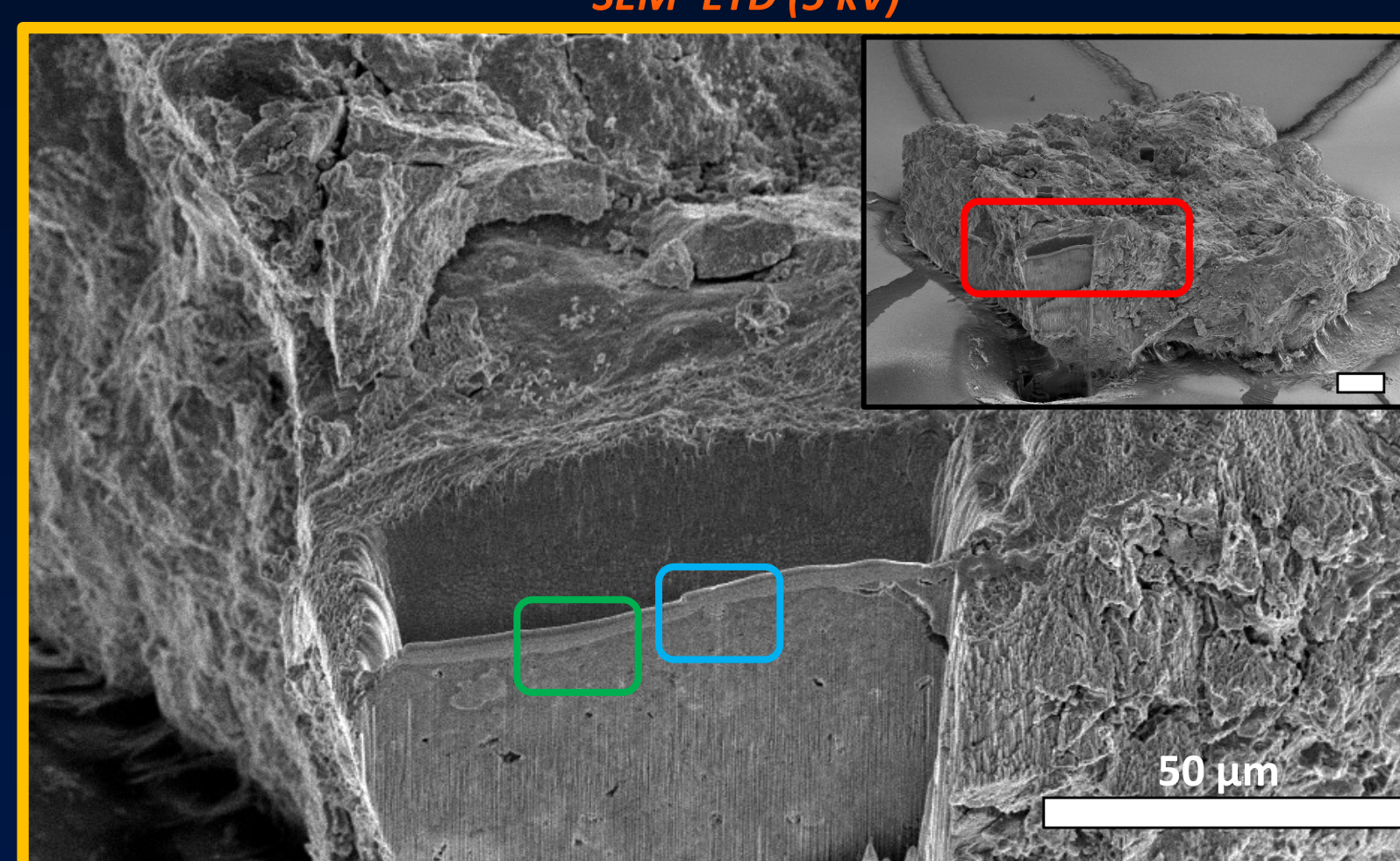


Figure 1: SE image of a grain of Ivuna on carbonate sticky and coated with 5 nm Au. Large cross section at the front of the grain was the location where 2 adjacent FIB lamella were extracted: one with C-K edge EELS then XANES (left extraction) and the other direct XANES (right lamella).

Lamella 2 – XANES first

SEM-ETD (2 kV)

STXM C map

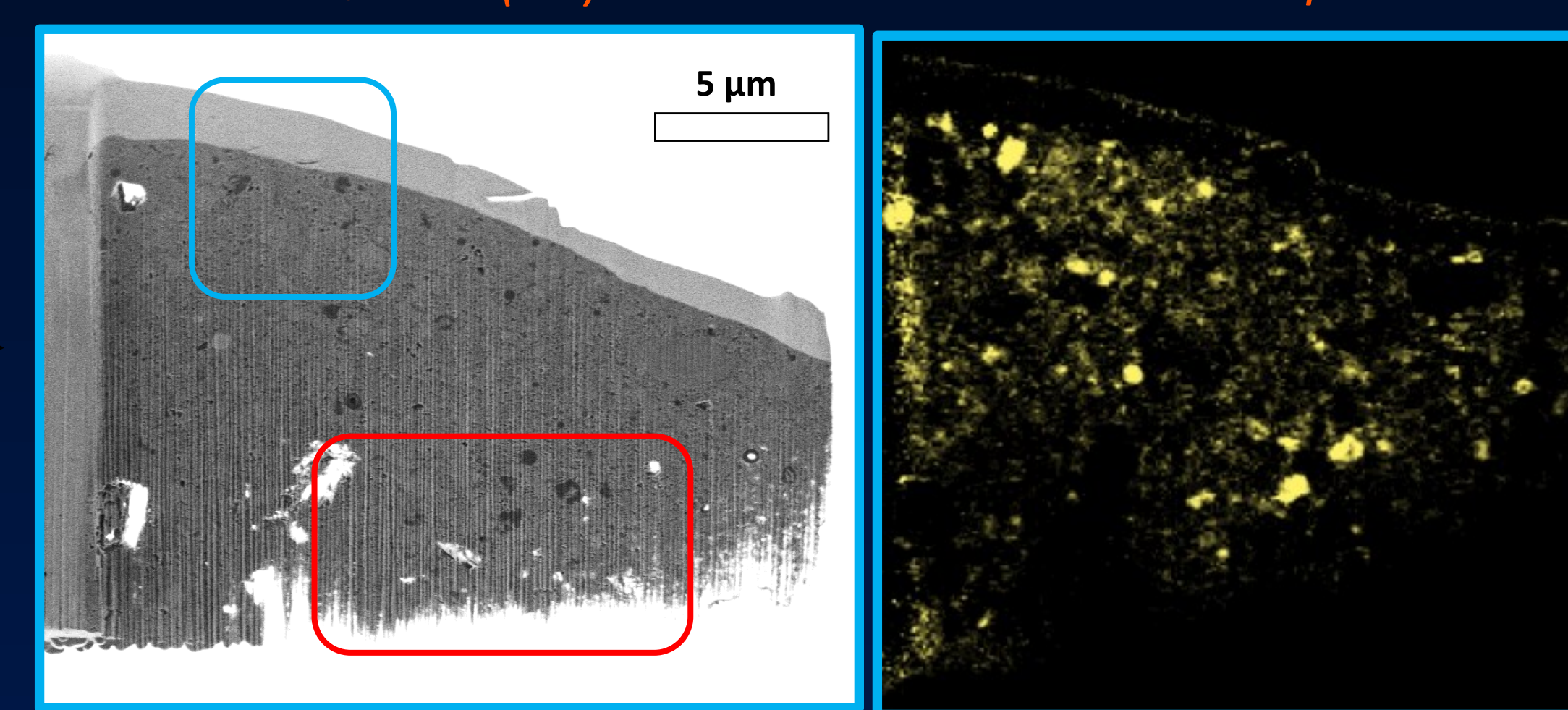


Figure 5: SE image (fast 5KV snap shot) of Ivuna lamella with XANES only. Right is a carbon map (OD 292 – 280 eV).

C K-α (EDS) C K-α EELS Thickness variability

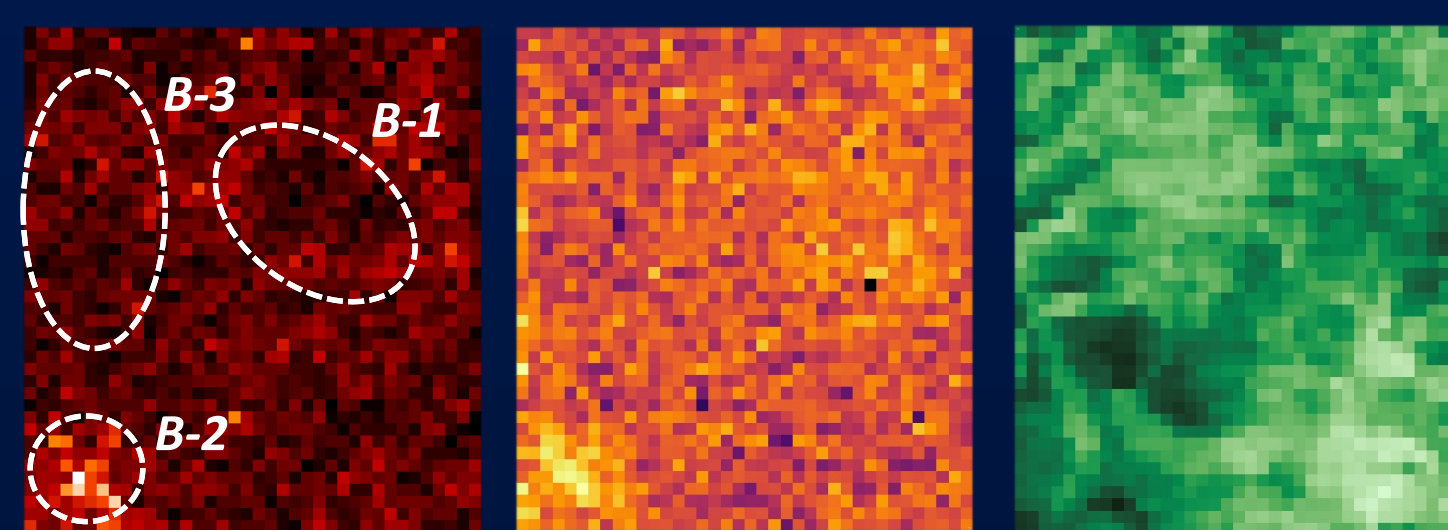
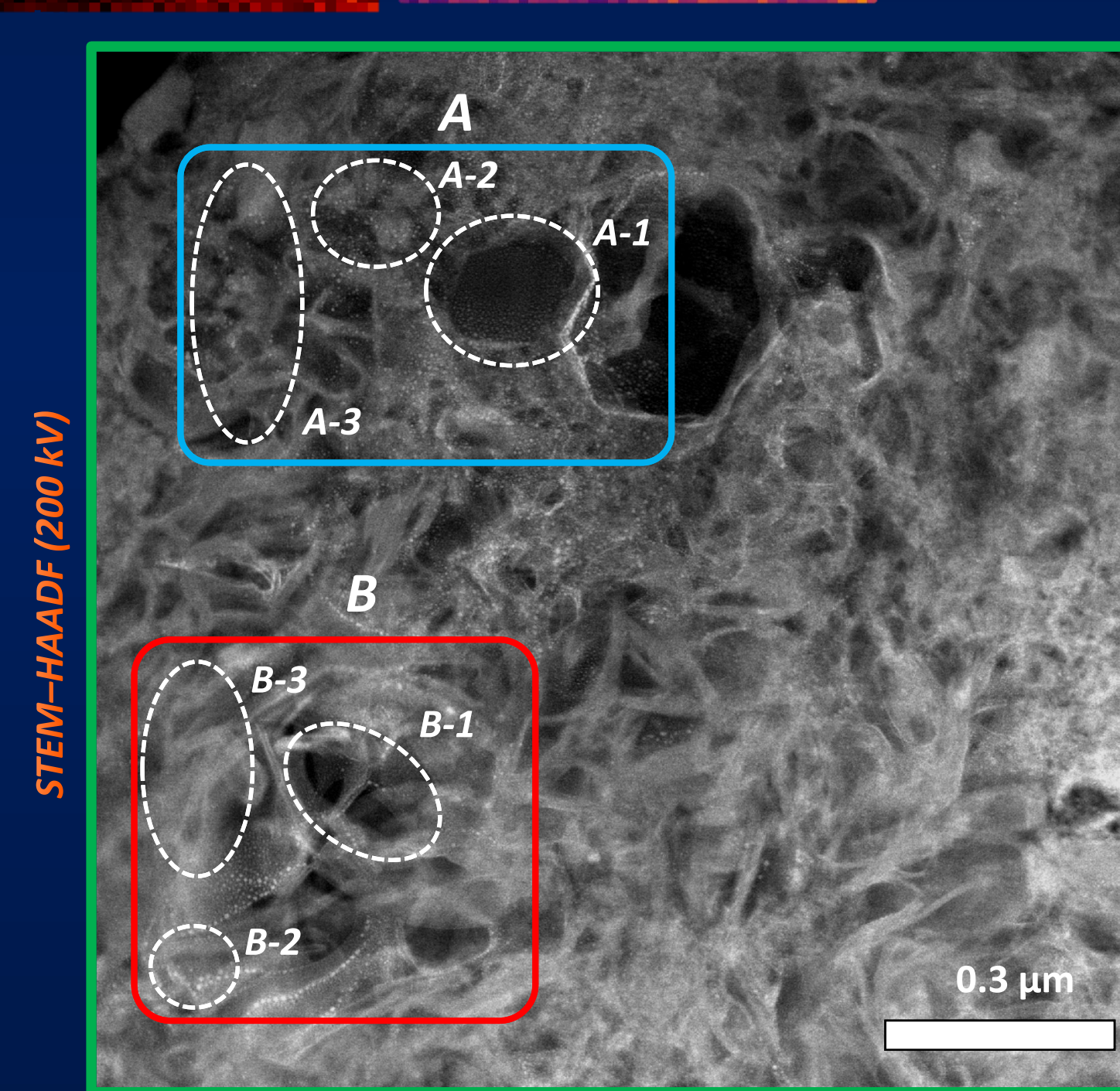
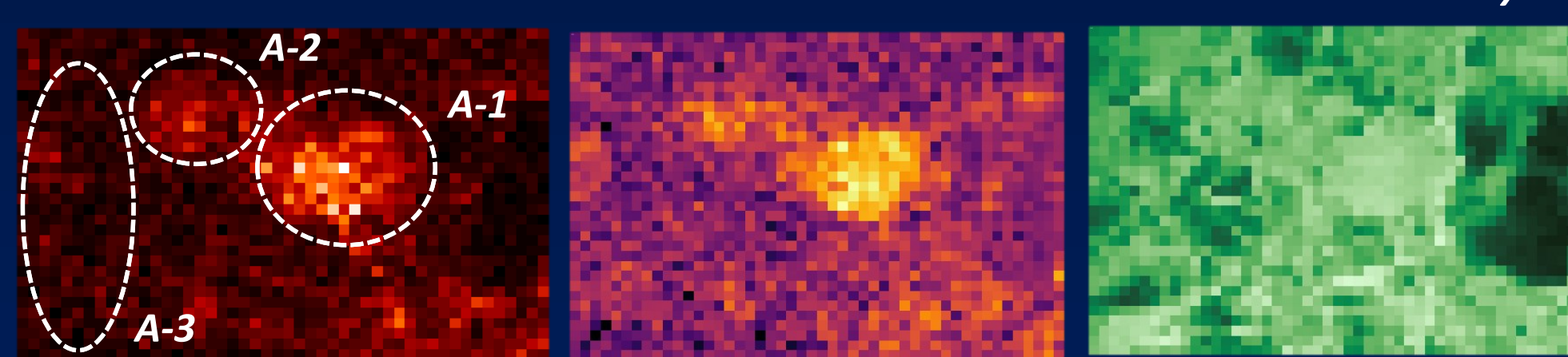


Figure 3: EELS of Organic particles and regions in phyllosilicate (diffuse OM [Le Guillou 2014]) are shown to the right.

STXM-XANES after TEM-EELS

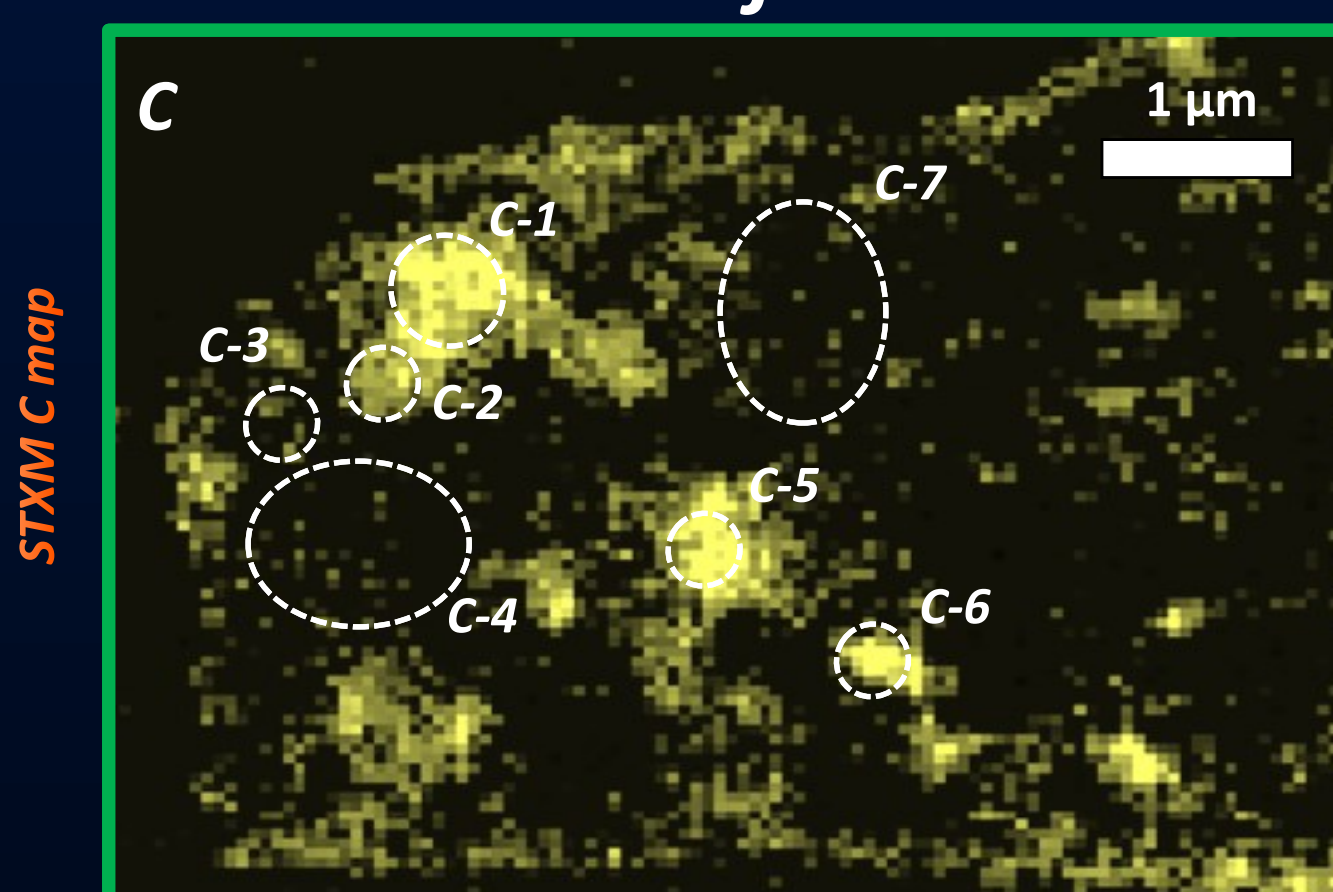
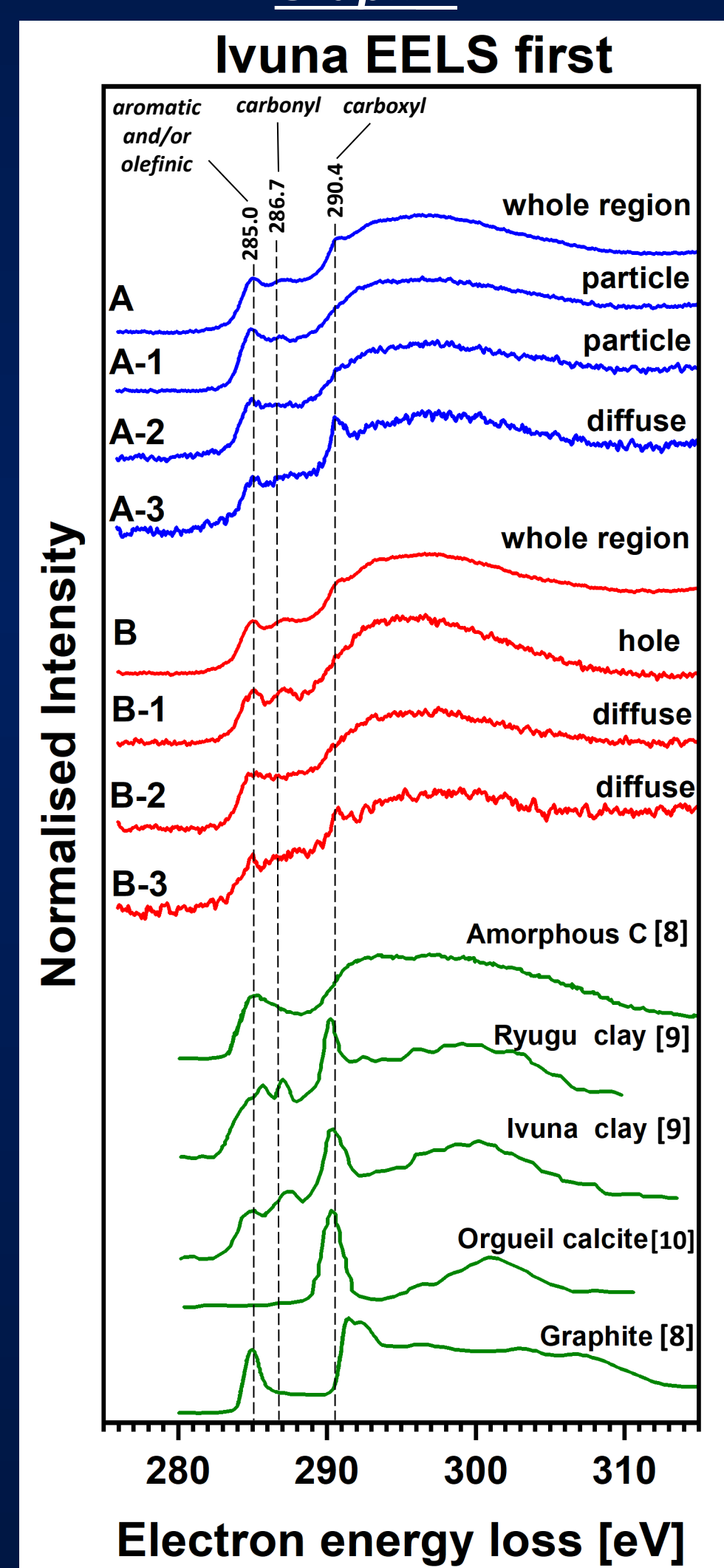
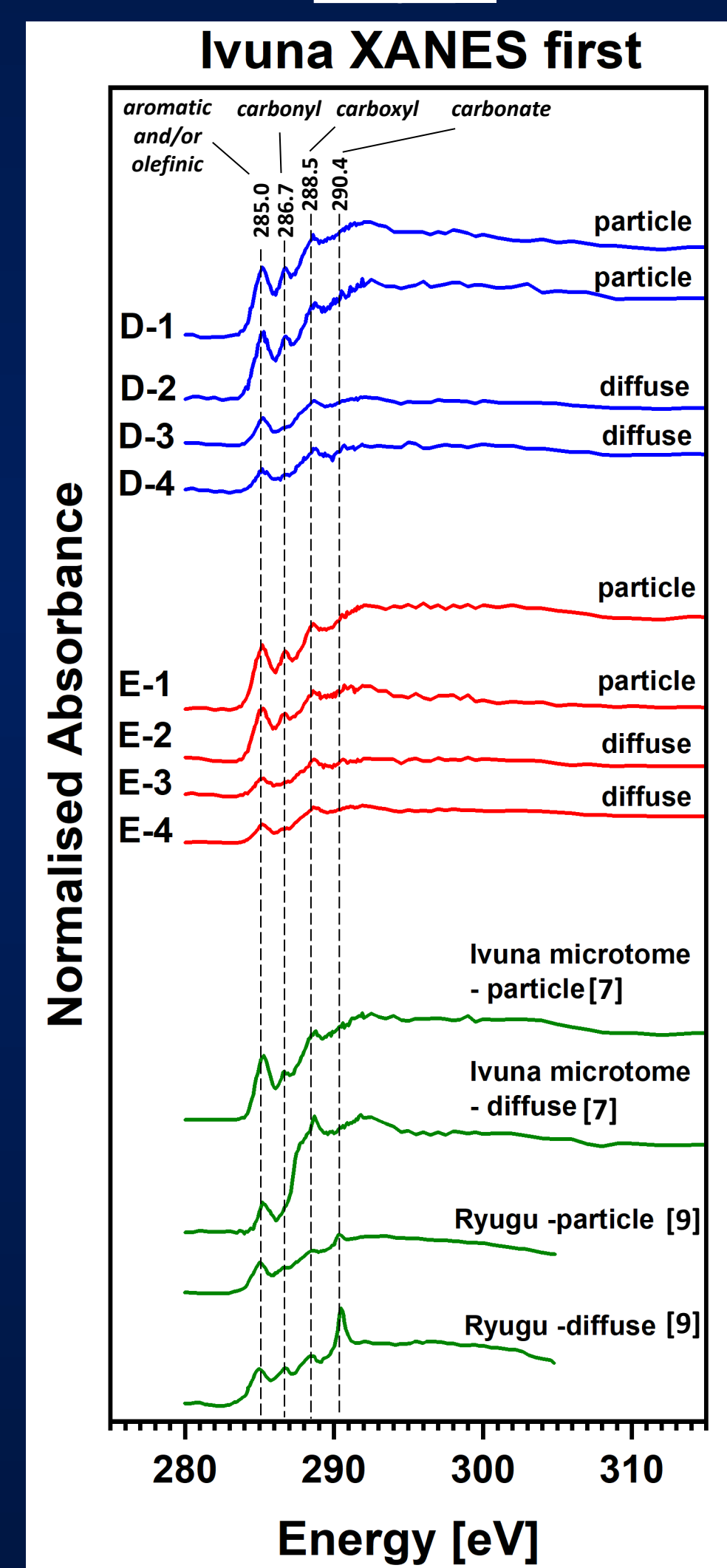


Figure 4: Optical Density (OD) carbon maps 292-280 eV of the lamella after S/TEM and EELS.

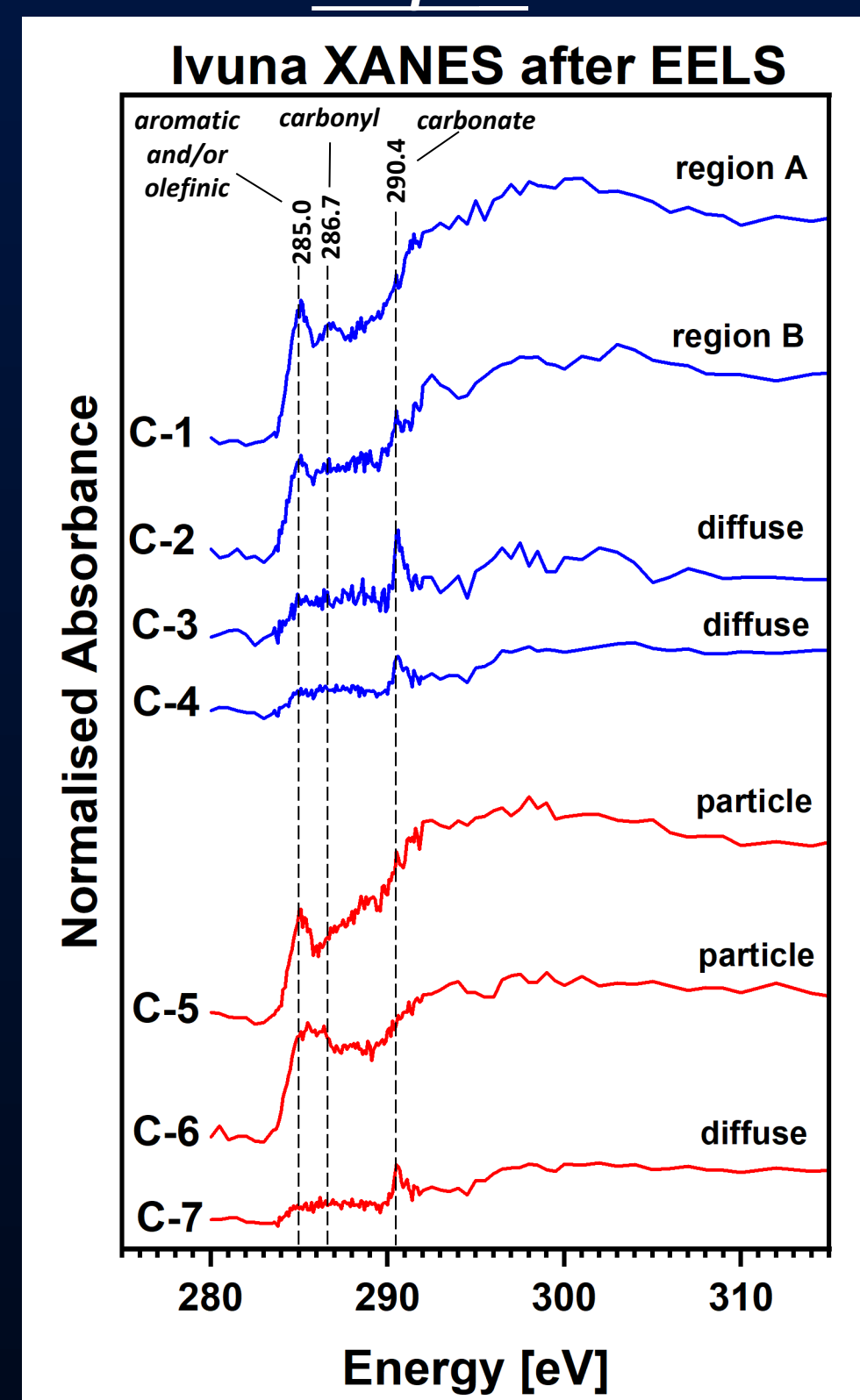
Graph 1



Graph 2



Graph 3



Graph 4

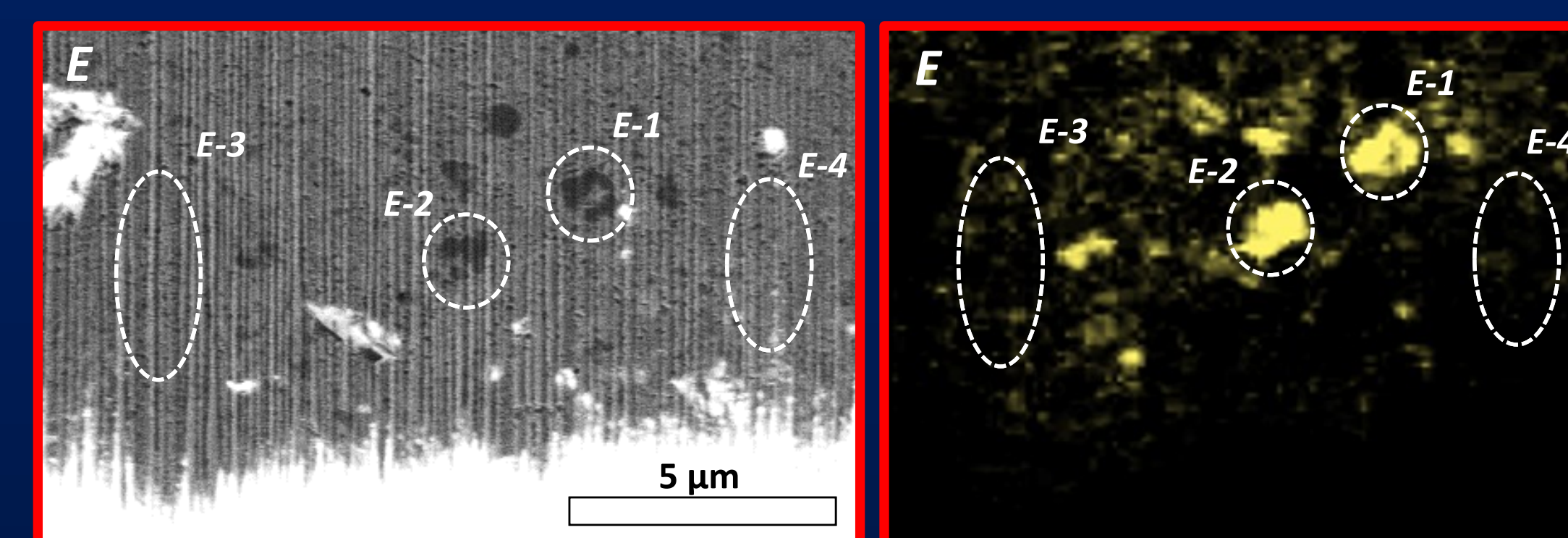
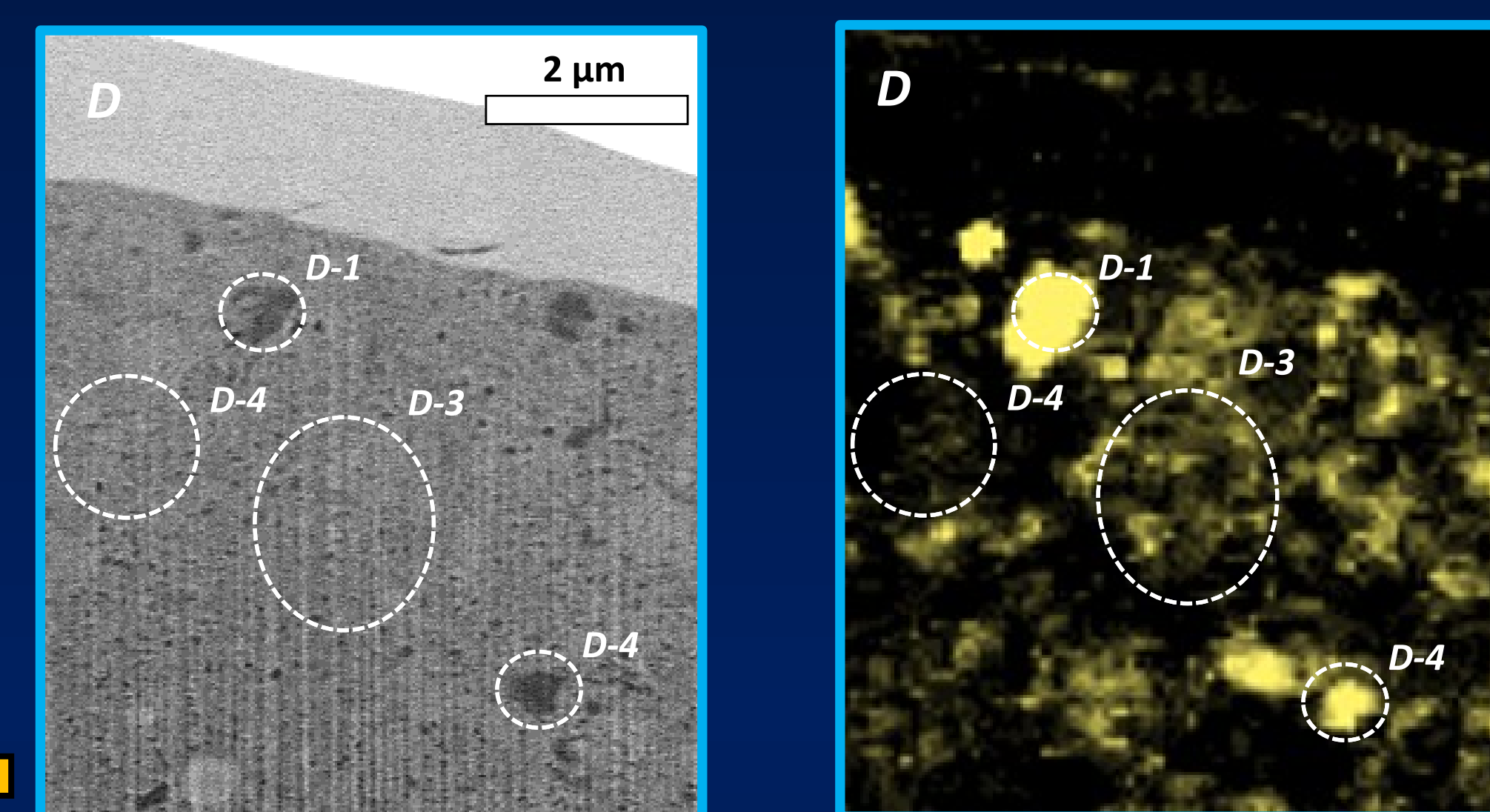
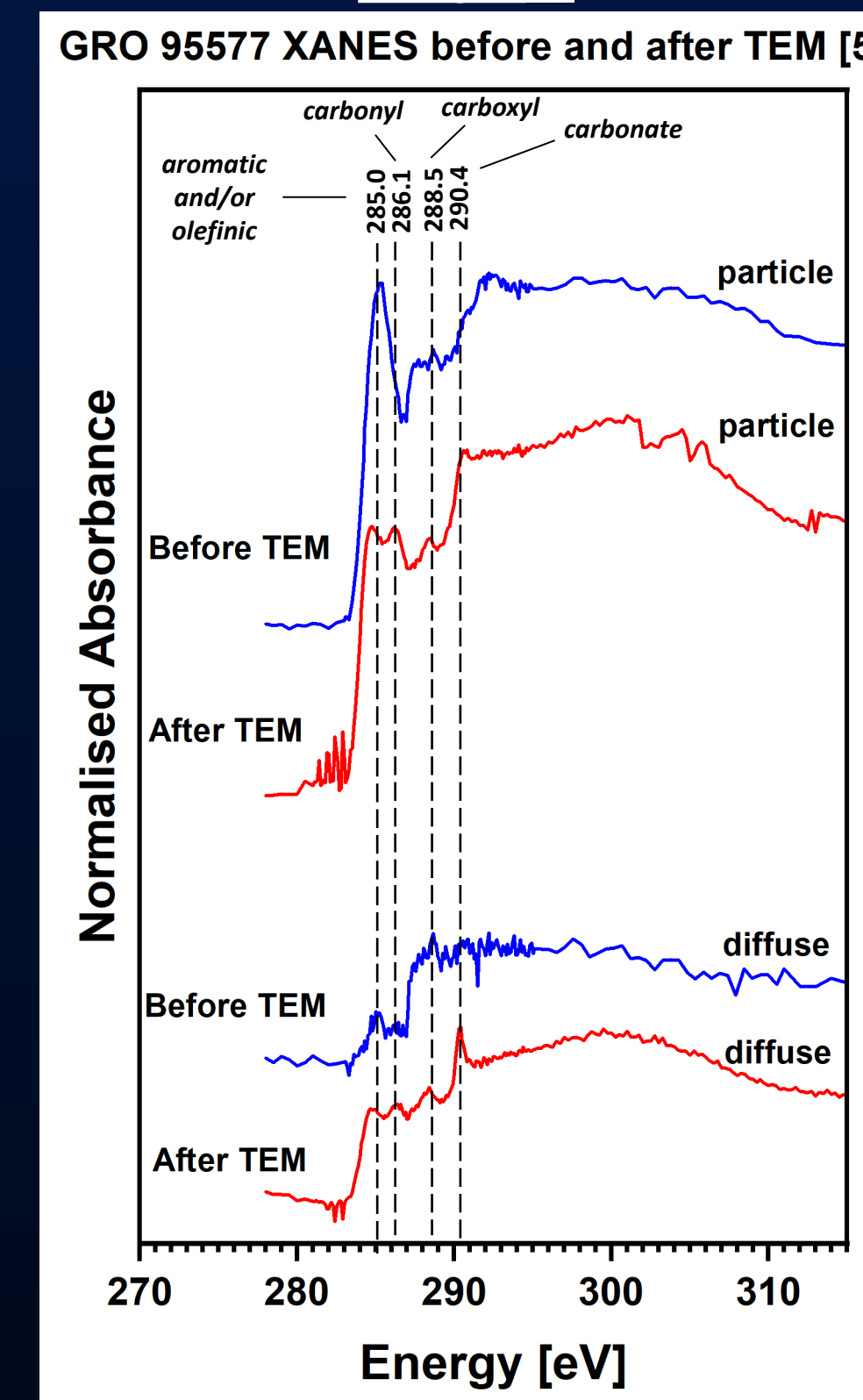


Figure 6: SE images with corresponding C maps (OD 292-280 eV) in 2 regions where the C-K edge XANES maps were made. Various extracted XANES ROIs are marked in the C maps.

STXM-XANES – TEM – STXM-XANES [5]

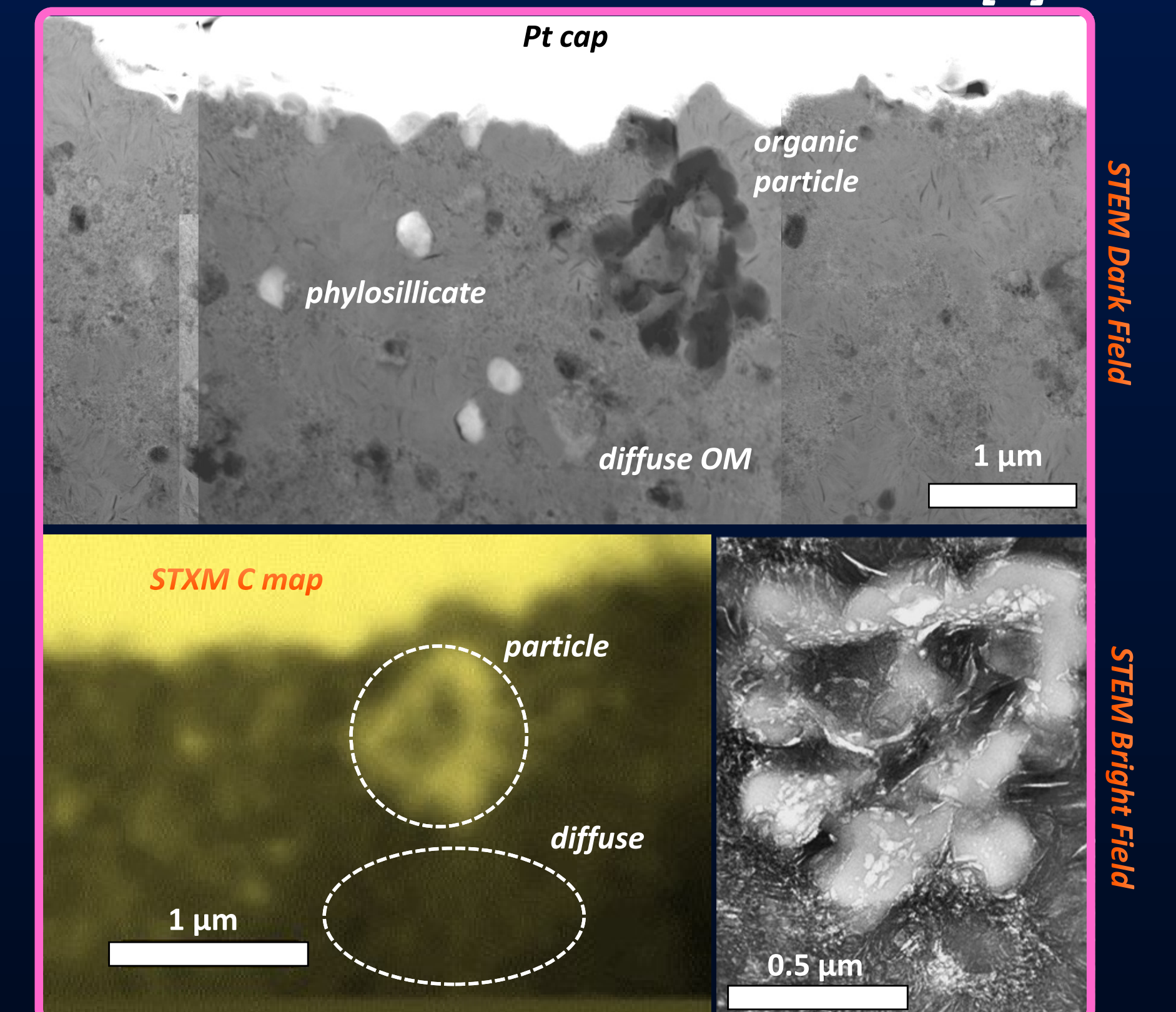


Figure 7: STXM-TEM of GRO 95577 (CR1), adapted from Changela et al. (2018). XANES spectra are extracted from the coarse organic particle and phyllosilicate ROI (diffuse OM) marked in the single energy 278 eV STXM image, prior to and post TEM. Left are the extract XANES. Note the distinct carbonate peak in the diffuse OM and organic particle post TEM analysis of the lamella.

Discussion

As shown in Graph 2 - XANES spectra from Lamella 2 [7] (no TEM-EELS), the aromatic-carbonyl-carboxyl (285.0 - 286.7 - 288.5 eV) particles and aromatic-poorer and carboxylic-rich diffuse OM are in good agreement with the previous studies [5, 6]. They are also consistent with XANES of a microtome sample of Ivuna (i.e. no FIB-SEM) [7]. Note that Lamella 2 experienced a 2 kV SEM snapshot at the end of final FIB polishing.

On the other hand, EELS results of both the organic particles and diffuse OM in Lamella 1 (Graph 1), as well as subsequent XANES of the same regions (Graph 3), show variation in organic functional chemistry and structure. EELS and XANES after TEM-EELS display the aromatic (285.0 eV) and carbonyl (286.7 eV) peaks in the particles, but lack the carboxylic (288.5 eV) peak. The carboxylic energy region is overlapped by a bulge similar to XANES of amorphous C [8]. The carboxylic peak characteristic of XANES of chondritic OM could be either completely replaced by or convoluted by increased σ^* amorphous C bulge peak (~288 – 315 eV). This means that TEM-EELS has changed the functional chemistry at least of indigenous macromolecular organic material. In case of the diffuse OM (within phyllosilicate), which have a strong carboxylic peak, both EELS and XANES after TEM-EELS show this peak to be absent and replaced by an ~290.4 eV peak corresponding to carbonate, implying that e-beam probably oxidised carboxy-bonds to carbonates ones. The same effect is also seen from the XANES spectra extracted from non-EELS regions (C5, C6 and C7), indicating its formation by TEM imaging alone without EELS. This is further supported by results from XANES-TEM-XANES (see Graph 4, Fig. 7) on lamella from GRO 95577 CR1 chondrite [5]. After extensive TEM on both organic particles and over phyllosilicate where diffuse OM occurs, XANES shows the formation of carbonate-bonds in both types of OM, but particularly noticeable in the diffuse OM.

The amount of radiation damage has been shown much lower in STXM-based XANES spectroscopy than in TEM-based EELS (e.g. [11], [12]). Our observations particularly of organo-carbonate bonds in diffuse OM shows its formation sensitive to e-beam exposure rather than X-ray exposure. Furthermore, Yabuta et al 2023 [9] reported the lack of any carbonate peak in microtome samples measured by XANES, but occurring in FIB sections with organic particles and diffuse OM (referred to as clay bound OM in their study of Ryugu samples). Our microtome samples of CI chips have also not identified this peak in any XANES measurements, suggesting that e-beam exposure during FIB-SEM preparation could also form organo-carbonate bonds observed in previous studies [5], [6] and [9].

Conclusion and future work

Electron beam exposure by TEM and EELS on chondritic OM changes its functional chemistry, in both its macromolecular and soluble/insoluble diffuse form in phyllosilicate. A bulge in the EELS spectra consistent with amorphous carbon σ^* peak (~288 – 315 eV) is found in organic particles. Carboxylic (288.5 eV) functional chemistry is replaced by organo-carbonate (290.4 eV) ones in the case of diffuse OM (phyllosilicate regions). This means that synchrotron XANES coordinated with subsequent TEM provides a more accurate characterisation of the functional chemical variation of OM *in situ* than EELS-TEM alone. Further work is required to test this via systematic SEM beam exposure to ultra thin samples during FIB-SEM sample preparation.

References

- [1] Sephton M. A. (2002), *Natural Product Report*, 19, pp. 292–311
- [2] Alexander C. M. O. et al. (2007), *Geochimica Cosmochimica Acta*, 71, pp. 4380–4403
- [3] Pizzarello S. et al. (2006), *Meteorites and the Early Solar System II*, 1, pp. 625–651
- [4] Glavin D.P. et al. (2018), in *Primitive meteorites and asteroids (chapter 3)*, pp. 205–271
- [5] Changela H. G. et al. (2018), *Meteoritics & Planetary Science*, 53, 1006–1029
- [6] Le Guillou C. et al. (2014), *Geochimica Cosmochimica Acta*, 131, 368–392
- [7] Changela H. G. (2023), *LPS Contributions*, Abstract 2848
- [8] Yuan J. & Brown L. M. (2000) *Micron* 31, pp. 515-525
- [9] H. Yabuta, et al. (2023), *Science*, 379, pp. 6634
- [10] Garvie L.A. & Buseck P.R. (2007) *Meteoritics & Planetary Science*, 42(12), pp. 2111-2117
- [11] Wang J. et al. (2009), *Journal of Electron Spectroscopy and Related Phenomena*, 170, pp. 25 – 36
- [12] Braun A. et al. (2009), *Journal of Electron Spectroscopy and Related Phenomena*, 170, pp. 42–48

Acknowledgments

- We acknowledge EP/PS/RES “Centre of Advanced Applied Sciences” (No. CZ.02.1.01/0.0/0.0/16_019/0000778)
- We thank Diamond Light Source for access and support in use of the electron Physical Imaging Centre (Instrument E01, proposal M630752) that contributed to the TEM-EELS-EDS results presented here. Particularly thank to Dr. Christopher Allen for his help.
- We thank TESCAN ORSAY holding a.s. for access and support in use of their instrumentation (Instrument FIB-SEM Amber X) used for Lamella 2 preparation. Particularly thanks to Dr. Hana Tesarova for her help.
- We thank CEITEC MUNI for access and support in use of their instrumentation (Instruments FIB-SEM FEI Versa 3D and FEI HELIOS 5 DualBeam) used for Lamella 1 preparation. Particularly thanks to Dr. Pavel Krepelka for his help.
- We thank KEK Photon Factory for access and support in use their instrumentation (Beamline BL 19A) that contributed to the STXM-XANES results presented here.